prosthesis

MDPI

Article

Decellularized Porcine Pericardium Enhances Autologous Vascularized Matrix as a Prosthesis for Left Ventricular Full-Wall Myocardial Reconstruction

Tanja Meyer [1,†], Serghei Cebotari [1,†], Gudrun Brandes [2], Dagmar Hartung [3], Frank Wacker [3], Monika Theis [1,†], Tim Kaufeld [1], Igor Tudorache [1,†], Ingo Nolte [4], Axel Haverich [1] and Tobias Schilling [1,*]

[1] Department of Cardiothoracic, Transplantation, and Vascular Surgery, Medical School Hannover, 30625 Hannover, Germany
[2] Institute of Cell Biology in the Center of Anatomy, Medical School Hannover, 30625 Hannover, Germany
[3] Institute for Radiology, Hannover Medical School, 30625 Hannover, Germany
[4] Clinic for Small Animals, University of Veterinary Medicine Hannover, Foundation, 30625 Hannover, Germany
* Correspondence: schilling.tobias@mh-hannover.de; Tel.: +49-511-532-6584
† Former student/employee of the department.

Abstract: Regenerative grafts for myocardial reconstruction are often mechanically not stable enough to withstand the left ventricle's high blood pressure. Hence, decellularized pericardium may serve as a stabilizing structure for biological myocardium prostheses. The efficacy of detergent- and enzyme-based protocols to decellularize porcine pericardium was compared. Then, the decellularized pericardium was employed for a primary cover of a transmural left ventricular defect in minipigs (n = 9). This pericardium patch was applied to mitigate the high-pressure load on an autologous stomach tissue, which was utilized as a regenerative tissue prosthesis. Decellularization of the porcine pericardium with deoxycholic acid (DOA)- and enzyme-based protocols (trypsin/EDTA) removed 90% of the original cells ($p < 0.001$). The trypsin/EDTA protocol significantly altered the matrix architecture compared to the DOA protocol. There were no infections or clinical signs of graft rejection following the transplantation of the decellularized pericardium and the autologous segment of the stomach in the surviving animals (n = 7). A good left ventricular function could be detected via MRI six months following surgery. The biological integration of the graft into the host's tissue was found histologically. The stabilization of initially fragile grafts with decellularized pericardium facilitates the application of regenerative myocardial prostheses even on the left ventricle.

Keywords: regenerative myocardial prostheses; transmural left ventricular reconstruction; cardiac surgery; decellularization of pericardium

Citation: Meyer, T.; Cebotari, S.; Brandes, G.; Hartung, D.; Wacker, F.; Theis, M.; Kaufeld, T.; Tudorache, I.; Nolte, I.; Haverich, A.; et al. Decellularized Porcine Pericardium Enhances Autologous Vascularized Matrix as a Prosthesis for Left Ventricular Full-Wall Myocardial Reconstruction. *Prosthesis* **2023**, *5*, 113–129. https://doi.org/10.3390/prosthesis5010010

Academic Editor: Raffaele Serra

Received: 20 December 2022
Revised: 14 January 2023
Accepted: 16 January 2023
Published: 1 February 2023

1. Introduction

Heart failure still causes a major burden of mortality and hospitalization worldwide, not the least because of the aging population and improved survivability of myocardial infarction [1]. Severe cases of heart failure can be treated by reconstructing the ventricle using the Dor procedure [2]. This procedure entails resecting dysfunctional, dilated ventricle areas to restore the best possible physiological volume and hemodynamically efficient heart geometry, directly affecting its pumping power [3]. Ideally, native, autologous pericardium is used as the prosthetic material in the Dor procedure [4,5]. However, there is not always a sufficient quantity of this tissue. Therefore, synthetic patch material such as Dacron is frequently used. Despite reducing the dilated left ventricle and a concomitant functional improvement in its pumping power, this method is still not optimal, because the synthetic materials have no regenerative potential, are incapable of growth, and do not have an active contractile function. Therefore, various approaches for regenerative bioprostheses have

been attempted to reconstruct or increase the function of the damaged myocardium [6]. In these studies, autologous tissue such as a matrix of jejunum [7], stomach [8], and decellularized bladder [9] or pericardium [10] was used to restore defects of myocardial lesions in animal experiments. In vivo remodeling was expected to form a functional intima and contractile tissue in the transplanted grafts. The migration of cardiomyocytes into the bioprostheses [7], the bioprostheses' connection to the coronary vascular system [8], and even a heartbeat-synchronous contraction were occasionally observed.

However, the experiments were mainly carried out on the right ventricle because the delicate biological grafts' mechanical stability is insufficient to withstand the high-pressure loads in the left ventricle. The rupture of a ventricular graft would result in the immediate death of the patient. Hence, biological grafts should have a greater layer thickness to provide enough mechanical stability. On the other hand, the supply of nutrients and oxygen-rich blood via diffusion is hardly sufficient in tissues with a layer thickness greater than 100 µm. In the case of stronger biomaterials, adequate vascularization is a prerequisite for the viability of the bioprostheses.

This pilot study aims to assess the feasibility of using a segment of autologous stomach (including its native vascular supply) to reconstruct a left ventricular transmural defect in a swine model. But first, pieces of allogeneic decellularized porcine pericardium are employed to primarily cover the defect, which mitigates the immediate, high-pressure load on the stomach graft. Reducing the load on the vascularized graft is carried out for its more physiological in vivo remodeling and, of course, preventing its rupture or the formation of aneurysms. The stomach is then fixed above the pericardium patch in a secondary step.

Because of the insufficient availability of autologous pericardium in the case of large-scale reconstructions in humans, decellularized xenogeneic pericardium could be a source of the patch material. Like the viable stomach tissue, it has the potential for a physiological transformation via repopulation with specific autologous functional cells. The grafts' in vivo repopulation requires preserving the pericardium's extracellular matrix during decellularization [11,12]. Therefore, in the first section of this study, porcine pericardium is decellularized with enzyme-based solutions or detergents. These protocols have been applied successfully to the decellularization of cardiac valves and vessels in prior experiments [13–16]. The decellularized pericardium will then be used to close the left ventricular transmural defect of the myocardium in swine. Additionally, the defect will be covered with an autologous and vascularized stomach segment. Stabilizing regenerative myocardial bioprostheses with a layer of decellularized pericardium opens promising therapeutic options other than cardiac transplantation or left ventricular assist devices for a plethora of patients with congestive heart failure.

2. Materials and Methods

2.1. Decellularization of Pericardium

Porcine pericardium was obtained from the local slaughterhouse. Samples were chilled at 4 °C in PBS (PBS tablets, Sigma-Aldrich Chemie GmbH, Taufkirchen, Germany), transported to the laboratory, stripped of fatty tissue, and divided into 1 cm^2 pieces.

In the first group, the pericardium was treated with deoxycholic acid (DOA) and sodium dodecyl sulfate (SDS) (DOA Group). The samples were incubated in 4% [w/v] sodium deoxycholate (Sigma-Aldrich Chemie GmbH, Taufkirchen, Germany) and 0.5% sodium dodecyl sulfate (Sigma-Aldrich Chemie GmbH, Taufkirchen, Germany) in distilled water with continuous shaking at ambient temperature for 60 min. They were then rinsed in PBS for 24 h. According to a previous study, the pericardium was decellularized by incubating twice in a trypsin/ethylenediaminetetraacetic acid (EDTA) solution (0.05% trypsin and 0.02% EDTA in PBS, Biochrom AG, Berlin, Germany) in a shaking water bath at 37 °C (shaking water bath 1083, Landgraf Laborgeräte, Langenhagen, Germany) for 24 h (trypsin/EDTA Group) [17]. After each incubation, the samples were rinsed in PBS at ambient temperature for 24 h. Native pericardium was used as the control group.

Penicillin/streptomycin (100 IU/mL penicillin and 100 µg/mL streptomycin, Biochrom AG, Berlin, Germany) were added to all rinses as antibiotic prophylaxis.

DNase I was applied to remove DNA fragments from the tissue after decellularization. The tissue was incubated in a shaking water bath at 37 °C for 90 min with 17 units of DNase I (Sigma-Aldrich Chemie GmbH, Taufkirchen, Germany) per ml of DNase I reaction buffer. It was then rinsed twice in PBS, shaking at 37 °C for 15 min.

2.2. Animal Experiment

The test animals were Lewe minipigs (n = 9) from the Ruthe Teaching and Research Farm of the University of Veterinary Medicine Hannover, Foundation. At the time of surgery, the average weight was 31.25 (SD: 3.1) kg.

2.3. Implantation

The surgery was performed under general anesthesia (20 mg ketamine/kg body weight i.m., B. Braun, Melsungen, Germany, and 2 mg Azaperone/kg body weight i.m., Janssen, Neuss, Germany) and with endotracheal intubation. The test animals received perioperative prophylaxis for arrhythmia (150 mg Amiodarone), pain (0.06 mL buprenorphine/kg body weight, Bayer, Leverkusen, Germany; 2 mg Carprofen/kg body weight, Pfizer, Berlin, Germany; 20 mg Metamizole/kg body weight, Intervet for three days), infection (5 mg metronidazole, Braun, Melsungen, Germany, for three days and 1 mL penicillin–streptomycin/50 kg body weight, AniMedica, Frankfurt, Germany, for four days), and gastric ulcers (40 mg Pantozol®, Nycomed, Konstanz, Germany). The surgery was a two-cavity operation in which, first, an approximately 4 × 4 cm piece of the stomach was resected via median laparotomy. This resection's native arterial and venous supply was preserved. The resulting wound in the stomach was closed with a continuous suture (PDS 2.0, Ethicon, Norderstedt, Germany). The heart was then connected to the cardiopulmonary bypass (Stöckert S3, Sorin Group Germany GmbH, Munich, Germany) via a left lateral thoracotomy in the fourth intercostal space. The cannulae were placed in the right atrium and the carotid artery. A systemic heparinization (400 IU/kg; heparin sodium 25,000, Ratiopharm, Ulm, Germany) and the initiation of cardiopulmonary bypass were then performed.

A transmural defect with a diameter of approximately 4 × 4 cm was set during cardiac arrest. This defect was initially covered by the decellularized allogeneic pericardium using a continuous suture (Polyprolene 4.0, Ethicon, Norderstedt, Germany). Subsequently, the prepared vascularized segment of the stomach was transdiaphragmatically displaced in the thoracic cavity, freed from the tunica mucosa, and fixed above the implanted pericardium on the heart muscle with single-button technology (Polyprolene 4.0, Ethicon, Norderstedt, Germany) (Figures 1 and 2).

The surgery was completed by antagonizing anticoagulation with protamine (400 IU/kg; Medapharma, Switzerland). The cannulae of the life-support machine were then removed. Finally, the ribs were fixed with non-absorbable sutures (Mersilene 2.0, Ethicon, Norderstedt, Germany), the skin was closed according to Donati's technique (CBX1 Vicryl, Ethicon, Norderstedt, Germany), and the wound was sealed with aluminum spray (Alma Pharm, Wildpoldsried, Germany).

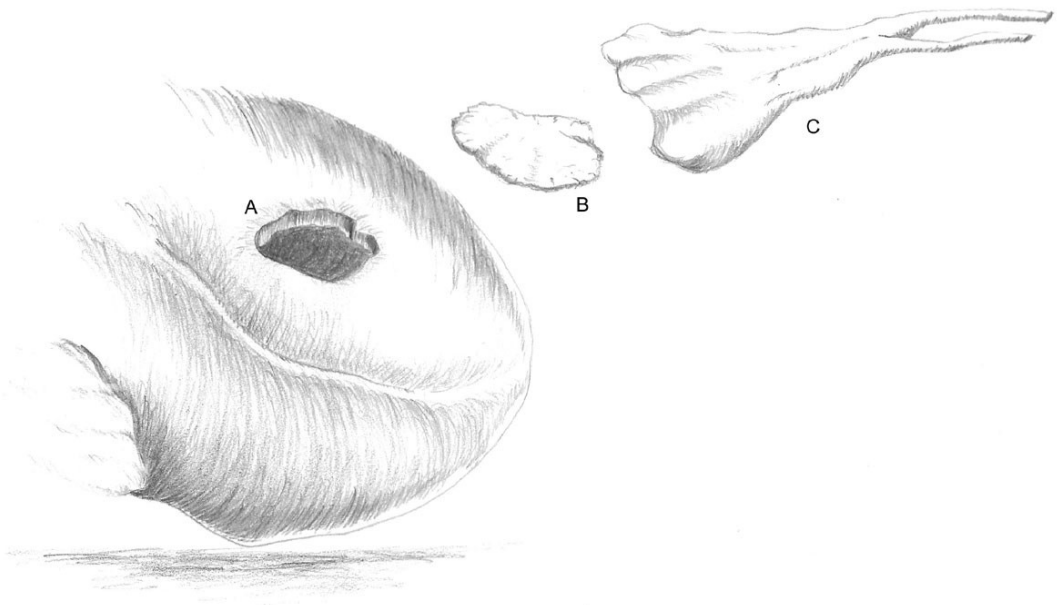

Figure 1. Schematic drawing of the surgical principle. First, excision of an annular segment of the left ventricular myocardium with a diameter of 4 cm. Second, suturing pericardium to an autologous vascularized patch of the swine's stomach. Third, transplantation of the pericardium–stomach construct onto the lesioned left ventricular myocardium. A: left ventricular lesion; B: pericardium patch; C: vascularized, autologous segment of the stomach.

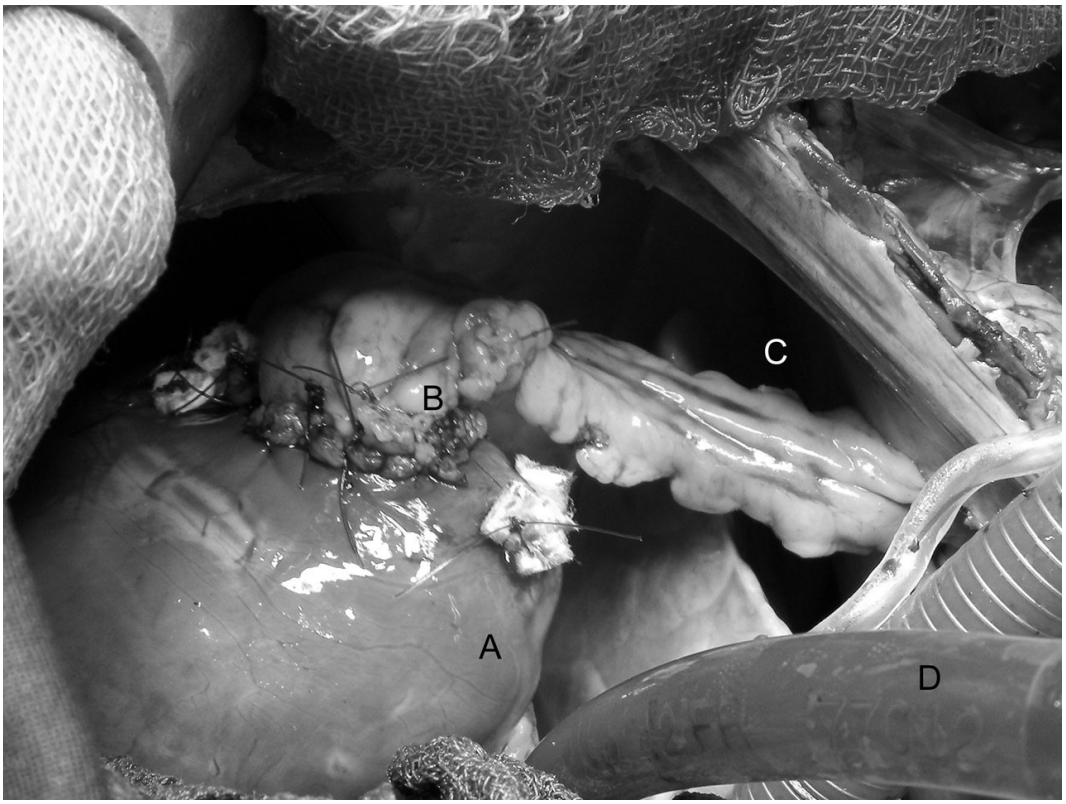

Figure 2. Intraoperative situs showing the implantation of a vascularized stomach segment in the left ventricular myocardium. A: cardiac apex; B: segment of the stomach with pedicle including native left gastroepiploic artery and vein above the patch of the decellularized pericardium; C: transdiaphragmatic passage; D: venous cannula.

2.4. Cardiac Magnetic Resonance Imaging (MRI)

The test animals were examined via MRI six months after the implantation and transplantation of the dual graft immediately before euthanasia. During the test, the pigs were sedated with Propofol Lipuro® i.v. (1 mL/kg KG/h, Braun, Melsungen, Germany), continuously ventilated, and placed in the MRI device in the left lateral position. The MRI scan was performed in a 1.5 Tesla MR scanner (Magnetom Avanto, Siemens Healthcare, Erlangen, Germany). During induced respiratory arrest, ECG-gated cine true fast imaging with steady-state precession (trueFISP) sequences were acquired. Two- and four-chamber images were generated. The inversion recovery (IR) trueFISP 2D sequence was used as delayed-enhancement (DE) imaging to assess the possible fibrosis areas. The recordings were made approximately 10 min after injecting an intravenous gadolinium contrast agent (Gadobutrol; Gadovist, Bayer Vital GmbH, Leverkusen, Germany) at a dose of 0.15 mmol/kg body weight.

A quantitative analysis of the left ventricular volume and function data was performed with CVI42 software, version 5.1.2 (Circle Cardiovascular Imaging Inc., Calgary, AB, Canada). The morphological characteristics, regional wall thickness, and wall motion were also assessed.

2.5. Explantation

The explantation of the heart was performed via a median sternotomy six months after the first surgery. First, the animals were intubated under general anesthesia, and adhesions between the epicardium, pericardium, stomach, and visceral pleura were dissolved. The minipigs were then euthanized via injection with pentobarbiturate (450 mg/kg body weight, WDT, Wertingen, Germany). After removing the hearts from the cadaver, the transplanted grafts (including a 1 cm wide rim) were taken from the myocardium and prepared for further studies.

2.6. Preparation for Histological Examination

2.6.1. Light Microscopy of the Decellularized Pericardium

Samples of the decellularized pericardium were fixed in 2.5% glutaraldehyde (Polysciences Inc., Warrington, PA, USA) in 0.1 M sodium cacodylate buffer (pH 7.3, Merck VWR, Darmstadt, Germany) at 4 °C for 12 h and then re-fixed as 1 mm^2 pieces in 2% osmium tetroxide (Polysciences, Warrington, PA, USA) in 0.1 M sodium cacodylate for 1 h. The samples were then dehydrogenated in an ascending ethanol series (25, 50, 75, 90, 100%, Mallinckrodt-Baker, Griesheim, Germany), embedded with toluene (Merck VWR, Darmstadt, Germany) in epoxy resin (Serva Electrophoresis GmbH, Heidelberg, Germany), and polymerized at 40 °C for 20 h and 60 °C for 40 h.

Semi-thin (1 µm) sections were made from the embedded samples using an ultramicrotome (Ultracut, Reichert-Jung, Vienna, Austria). These showed the tissue in cross-section. In distilled water, they were stained with 1% toluidine blue (Merck) and 1% disodium tetraborate (Riedel de Haen AG, Seelze, Germany).

2.6.2. Scanning Electron Microscopy of the Decellularized Pericardium

The decellularized samples were dehydrated in an ascending acetone series (30, 50, 70, 90, 100%, Merck VWR, Darmstadt, Germany). The critical-point drying was performed in a critical-point-drying apparatus (CPD030, BalTec, Balzers, Liechtenstein). The samples were then coated with a 30 nm gold–palladium layer using a cathode-sputtering device (Sputter Coater E5000RT, Polaron Equipment LTD., Watford, England).

The surface of the samples was then examined under a scanning electron microscope (SEM 505, Philips, Eindhoven, The Netherlands).

2.6.3. Biometric Assessment of the Cell Density and Collagen Architecture of the Decellularized Pericardium

The existing cells and cell debris in the connective tissue of the decellularized pericardium were counted using ready-made toluidine blue preparations. The randomized and anonymized sample was counted using ImageJ software (National Institutes of Health, Bethesda, MD, USA). The results are given as the number of cells per 100,000 μm^2.

The space between the collagen fiber bundles, as well as the density of the fibers in the bundle, were evaluated to assess the quality of the extracellular matrix.

The randomized and anonymous evaluation was carried out by two people independently, and the results were averaged.

2.6.4. Overview of the Staining and Immunohistochemistry of the Explants

The samples were fixed in 3.5% formaldehyde solution (Otto Fischer GmbH & Co. KG, Saarbrücken, Germany), dehydrated in alcohol solutions of increasing concentration, and embedded in paraffin (Carl Roth GmbH & Co. KG, Karlsruhe, Germany). Finally, 10 µm thick sections were stained with Movat Pentachrome (Merck KGaA, Germany, and Waldeck GmbH & Co. KG, Münster, Germany).

Samples of the explant were fixed and frozen at −70 °C in Tissue Tek (Sakura Finetek, Torrance, CA, USA) for the immunohistological diagnosis. Double-staining with different antigen specificity for troponin T and the smooth muscle of the stomach tissue and the myocardium was carried out to differentiate between the smooth-muscle myosin heavy-chain proteins. The general cell staining was carried out using 4′,6-diamidine-2-phenylindole (DAPI).

2.7. Statistical Analysis

The statistical analyses were performed using SPSS 24 software (SPSS Inc., Munich, Germany). The variables were compared with a *t*-test for non-connected samples. The significance level was specified as $p < 0.05$; $p < 0.001$ is considered highly significant.

3. Results

3.1. Decellularization of Pericardium

3.1.1. Native Pericardium

The native pericardium was histologically and electron-microscopically used as a reference. On the surface, there was a nearly confluent mesothelium cell layer under which there was cell-rich connective tissue with capillaries and larger vessels (Figure 3A,B). The collagen fibers were a densely packed, closely knit bundle. In the longitudinal section, the fibers showed a wavelike configuration. Finer collagen fiber bundles were located in the sub-mesothelial regions of the tissue, whereas in the deeper layers of the tissue, the diameter of the bundle increased. The entire tissue was interspersed with irregularly arranged elastic fibers of variable widths (Table 1).

Table 1. Overview of major histological findings.

Treatment	Characterization	Collagen	Decellularization
Native	• Confluent mesothelial cell layer • Connective tissue cells • Capillaries and vessels	• Collagen fibers packed in dense bundles • Wavelike configuration • More delicate bundles in sub-mesothelial regions, thicker bundles in deeper layers • Irregularly distributed elastic fibers	n.a.

Table 1. *Cont.*

Treatment	Characterization	Collagen	Decellularization
Treatment	**Characterization**	**Collagen**	**Decellularization**
DOA	• Configuration and distribution of collagenous and elastic fibers like native tissue • Rare lesions of basal lamina	• Distance of fibers equal to native tissue	• Almost completely decellularized (up to 95% compared to native tissue)
Trypsin/EDTA	• Completely removed basal lamina to a greater extent than in DOA-treated tissues • Wavelike configuration preserved	• Greater distance and reduced density of collagen fibers compared to native and DOA-treated tissues	• Almost completely decellularized (up to 93% compared to native tissue) • No significant difference in cell count compared to DOA-treated tissues

3.1.2. Pericardium following Decellularization Procedures

After treatment with DOA and trypsin/EDTA, the cell number was reduced by approximately 90% compared with the native control specimens ($p < 0.001$) (Figure 3C,E and Figure 4, Table 1). The mesothelial surfaces of the samples from the DOA group showed a preserved basal lamina, which largely corresponded to the native findings (Figure 3D, Table 1). In contrast to this observation, in all pericardium samples treated with trypsin/EDTA, scanning electron microscopy revealed a fully exposed collagen fiber layer without residues of cells or the basal lamina (Figure 3F, Table 1).

In the trypsin/EDTA samples, the entire architecture of the collagen scaffold was altered compared to the samples of the other groups. There was increased space between the collagen fibers and a reduced density of the bundles. In the pericardium treated with DOA, wavy and parallel dense collagen fiber bundles were similar to the native pericardium (Figure 3A,C,E). Nevertheless, the distance between the collagen fibers was slightly increased in the DOA group compared with the native samples.

3.2. Clinical Results and Macroscopic Findings

Because of the effective yet gentle cell extraction via DOA, a piece of DOA-decellularized allogeneic pericardium was eventually used to cover the transmural myocardial lesion before the vascularized gastric patch was fixed epicardially. The operating time was, on average, 253.4 (SD 42.41) minutes (extracorporeal circulation time: 104.11 (SD 19.35) min; cardiac arrest time: 76.78 (SD 16.12) min). Two animals died perioperatively because of bleeding complications. The surviving test animals (n = 7) displayed normal eating and activity behavior during the six-month observation period without significant clinical complications. During explantation, the gastric patch imposed quite hypokinetically, but there was no evidence of a rupture or pathological aneurysm of the grafts or the adjacent myocardial zones. The area of the transplanted segment of the stomach (Figure 5A) was marked by strong connective tissue formation.

There was a confluent endothelialized surface on the luminal side of the implanted pericardium–stomach graft and no evidence of thrombus formation. The border zone between the native myocardium and graft consisted of solid white scar tissue with striated offshoots in the surrounding endocardium (Figure 6).

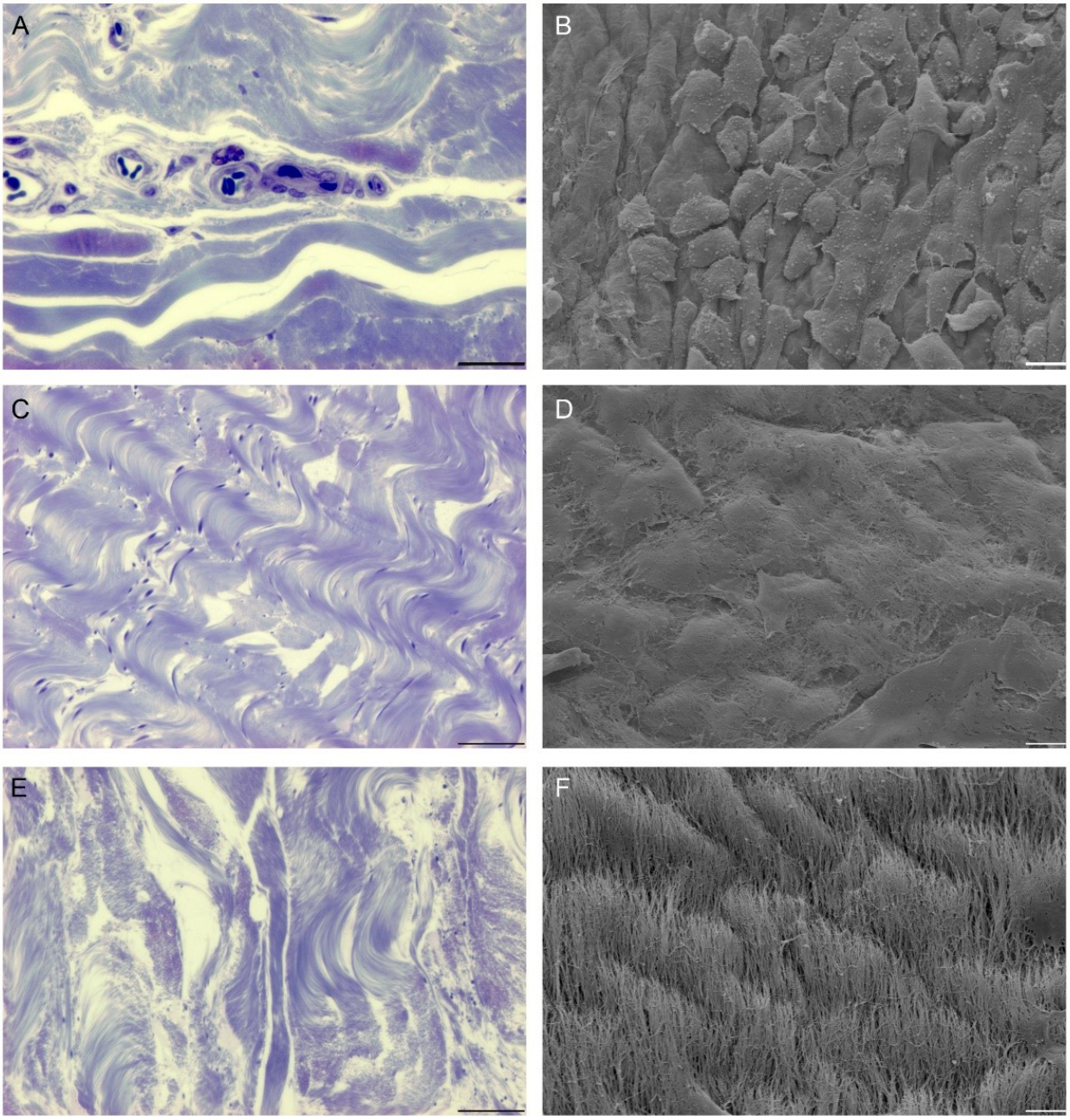

Figure 3. Histological findings of the porcine pericardium. Left column: toluidine blue staining; the black bar indicates 100 µm. Right column: scanning electron microscopy; the white bar indicates 10 µm. (**A** + **B**): native pericardium; (**C** + **D**): pericardium treated with DOA; (**E** + **F**): pericardium treated with trypsin/EDTA.

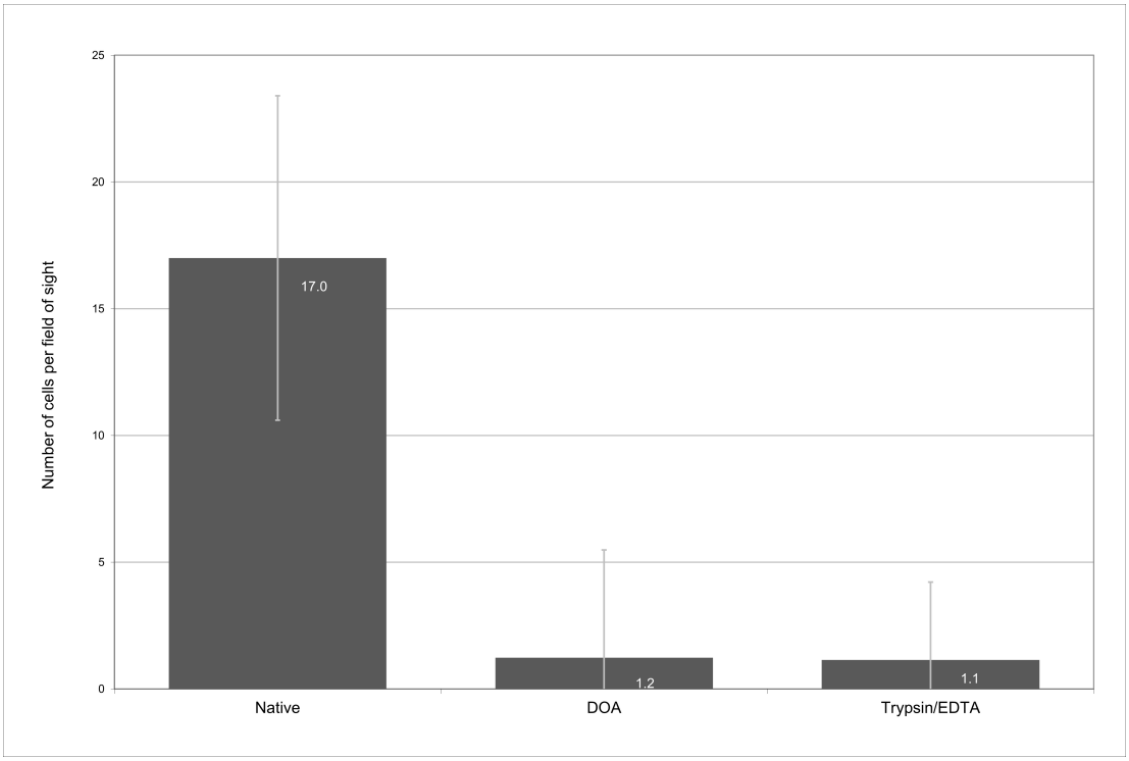

Figure 4. Histological analysis: number of cells of native and decellularized pericardium per 100,000 μm^2.

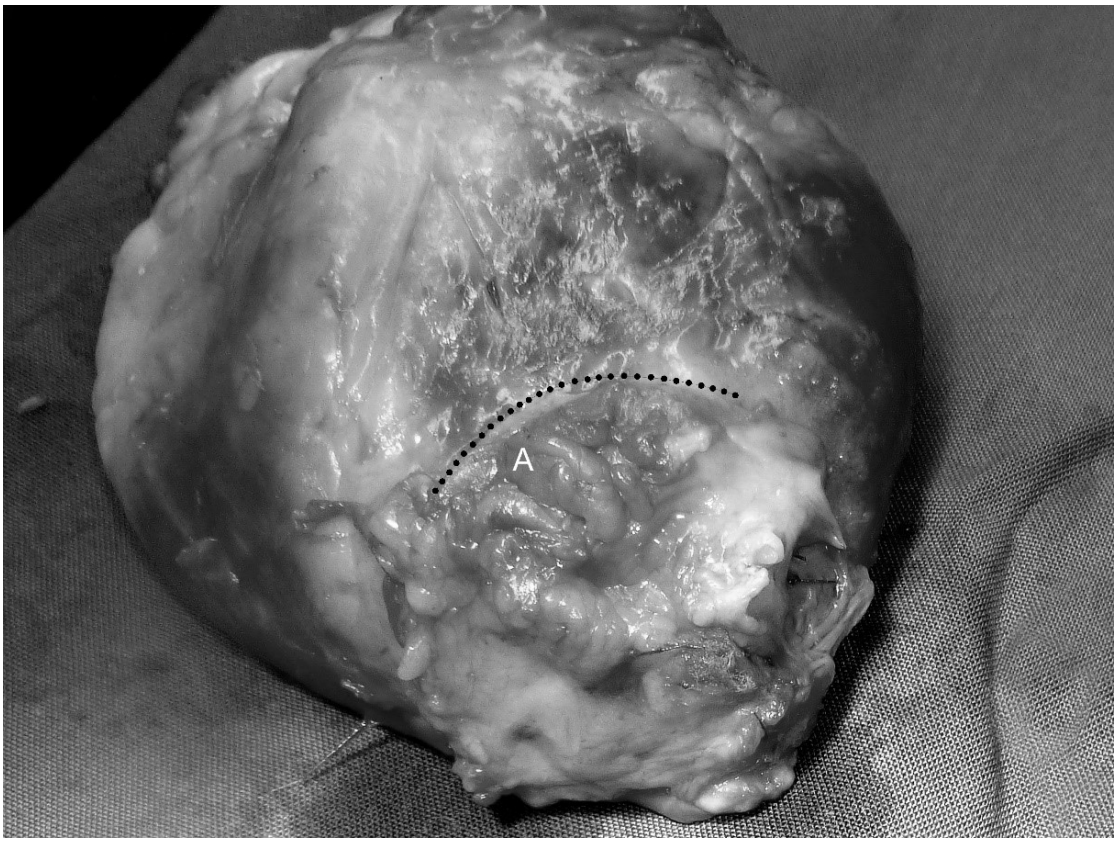

Figure 5. Explanted heart, including the patch of the decellularized pericardium and autologous vascularized stomach (delineated from the native myocardium by the dotted line, which lies within the cicatricial tissue in the border zone between host tissue and graft) without formation of an aneurysm (A).

3.3. MRI

Overall, the left ventricles were of normal size. The area of the implanted patch and the surrounding zone of the myocardium were functionally stable without rupture or aneurysm of the tissue (Figure 7C,D). Compared with the properly contracting healthy myocardium on the opposite side, akinesia was detected in the central patch area (Figure 7C,D) and hypokinesia in the border zone of the patch. A slight increase in wall thickness was seen in the edge region of the patch during the end-systolic and end-diastolic phases (Figure 7A,B), which was less prominent than in the native, opposite side of the ventricle (Figure 7C,D). Overall, the patch area demonstrated an inhomogeneously delayed enhancement of the contrast agent, indicating a stabilizing fibrosis (Figure 7E).

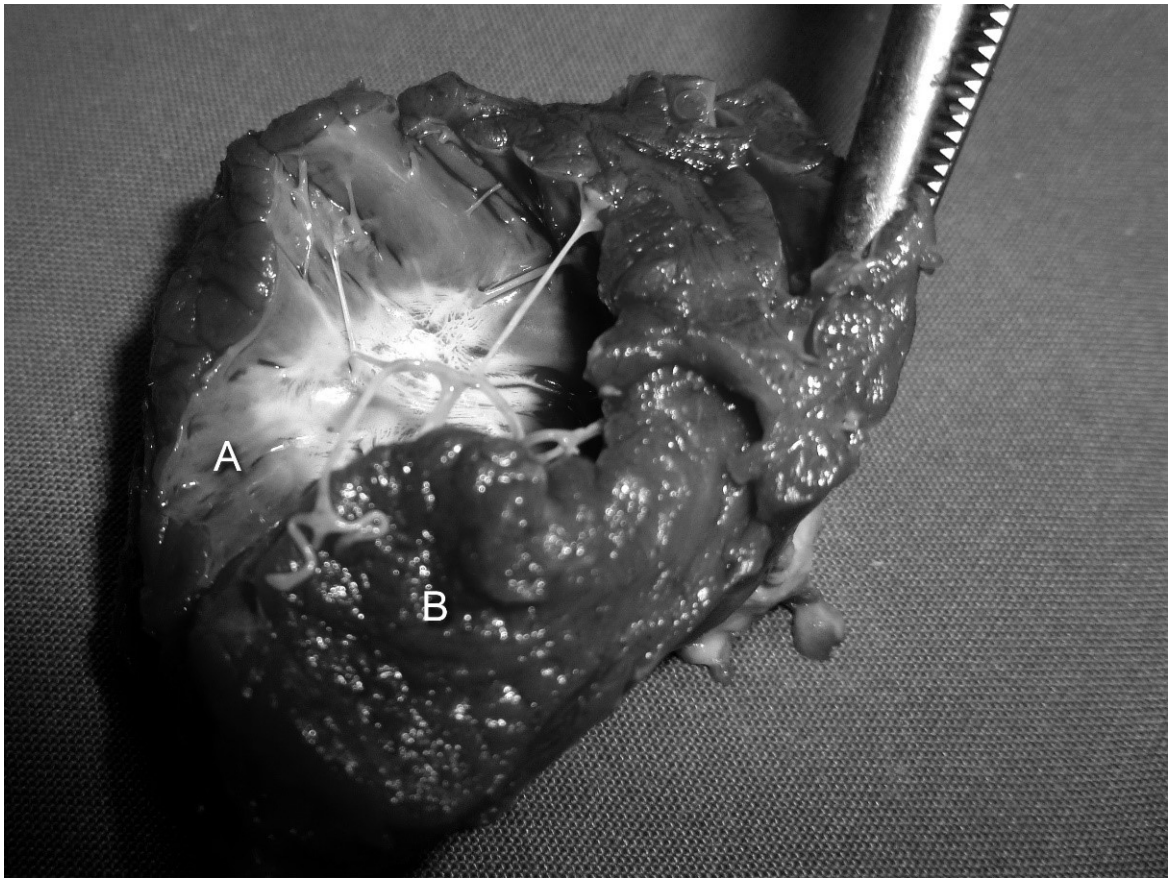

Figure 6. Luminal view of the explanted patch of the decellularized pericardium and an autologous vascularized stomach segment (A), surrounded by left ventricular myocardium (B). Smooth and confluent endocardium, no signs of thrombogenesis, no rupture or aneurysm of the graft.

3.4. Histology and Immunohistochemistry of the Explanted Grafts and Myocardium

Good integration of the myocardium, the implanted pericardium, and the gastric patch could be seen six months following surgery (Figure 8). The granulation tissue, which indicates graft integration into the host's tissue, was differentiated from the native myocardium, characterized by its typical striation of cardiomyocytes. Numerous capillaries and smaller vessels were found in the border zone between the graft and the native myocardium (Figure 8B). The multi-layer structure of the stomach wall was preserved. However, the applied pericardium could not be differentiated from the host's cardiac and gastric structures (Figures 8 and 9). The luminal side of the graft was covered with a confluent layer of endothelial cells. Signs of necrosis, early degeneration, or thrombus formation were not seen.

From an immunohistological perspective, the myocardium remained clearly delineated from the implanted pericardium and stomach segment. Differentiation of the pericardium from the cicatricial tissue was immunohistochemically impossible. Overall, numerous cell nuclei could be stained in the graft tissue that epicardially bordered the myocardium six months after implantation. In all areas, there were capillaries and blood vessels.

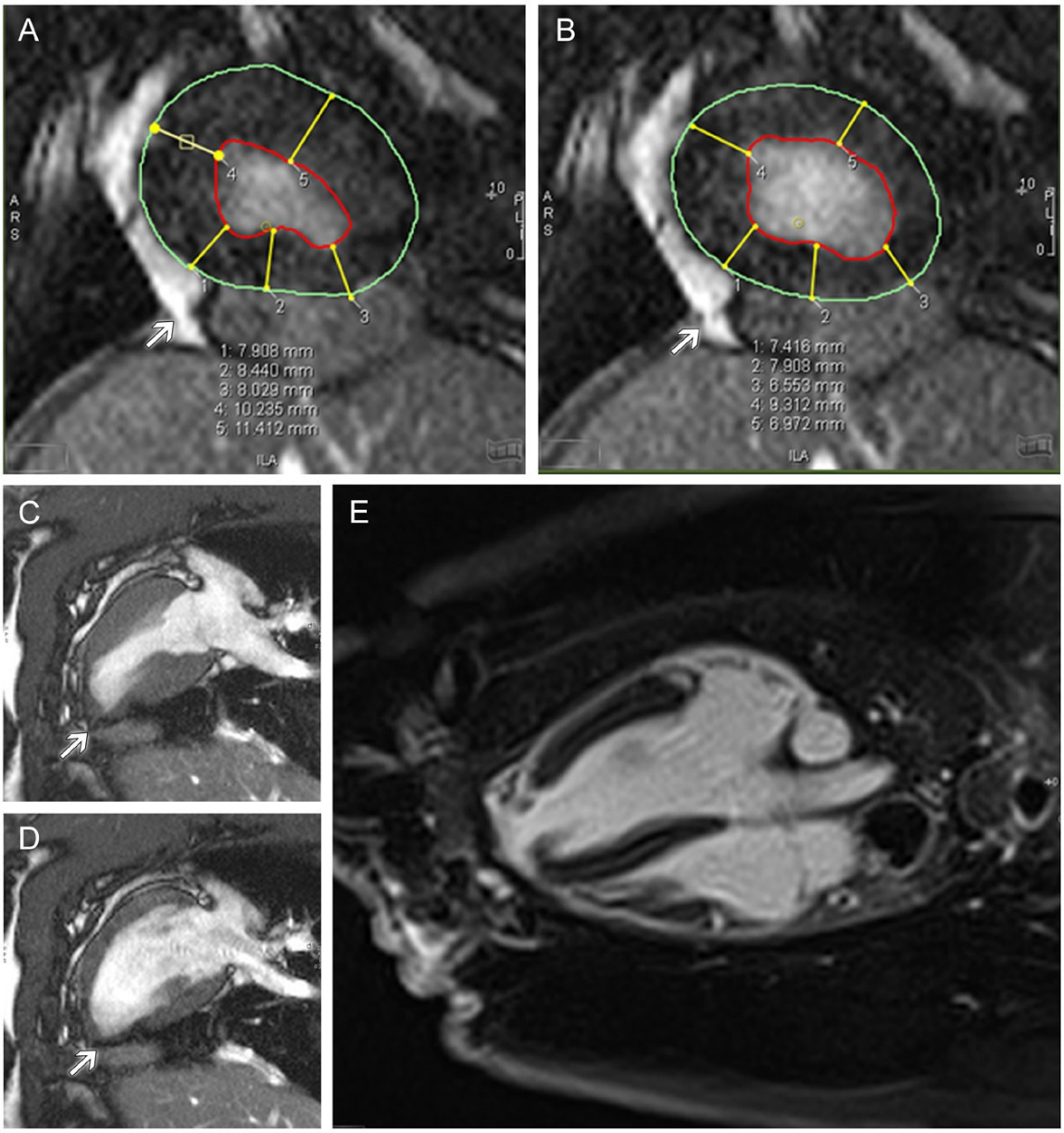

Figure 7. (**A** + **B**): MRI measurement of end-systolic (**A**) and end-diastolic (**B**) wall thickness of left ventricular myocardium. (**C** + **D**): MRI of the left ventricle as a two-chamber view during systole (**C**) and diastole (**D**) showing akinesia of the central region of the decellularized pericardium and stomach patch as well as hypokinesia of the peripheral areas. (**E**): MRI of the left ventricle as a four-chamber view close to the apex cordis with delayed enhancement indicating fibrosis (light grey) in the patch area in contrast to native myocardium (dark grey). Arrows indicate the area of the implanted stomach tissue. The end-diastolic volume of the left ventricle, including the gastric patch, was in a normal range compared with a healthy control animal with an average left ventricular ejection fraction of 54%. The volumes and function values of the right ventricle were also in the normal range (RV-EDV: 40 mL; RV-ESV: 18 mL; RV-SV: 23 mL; RV-EF: 56%; muscle mass: 20 g).

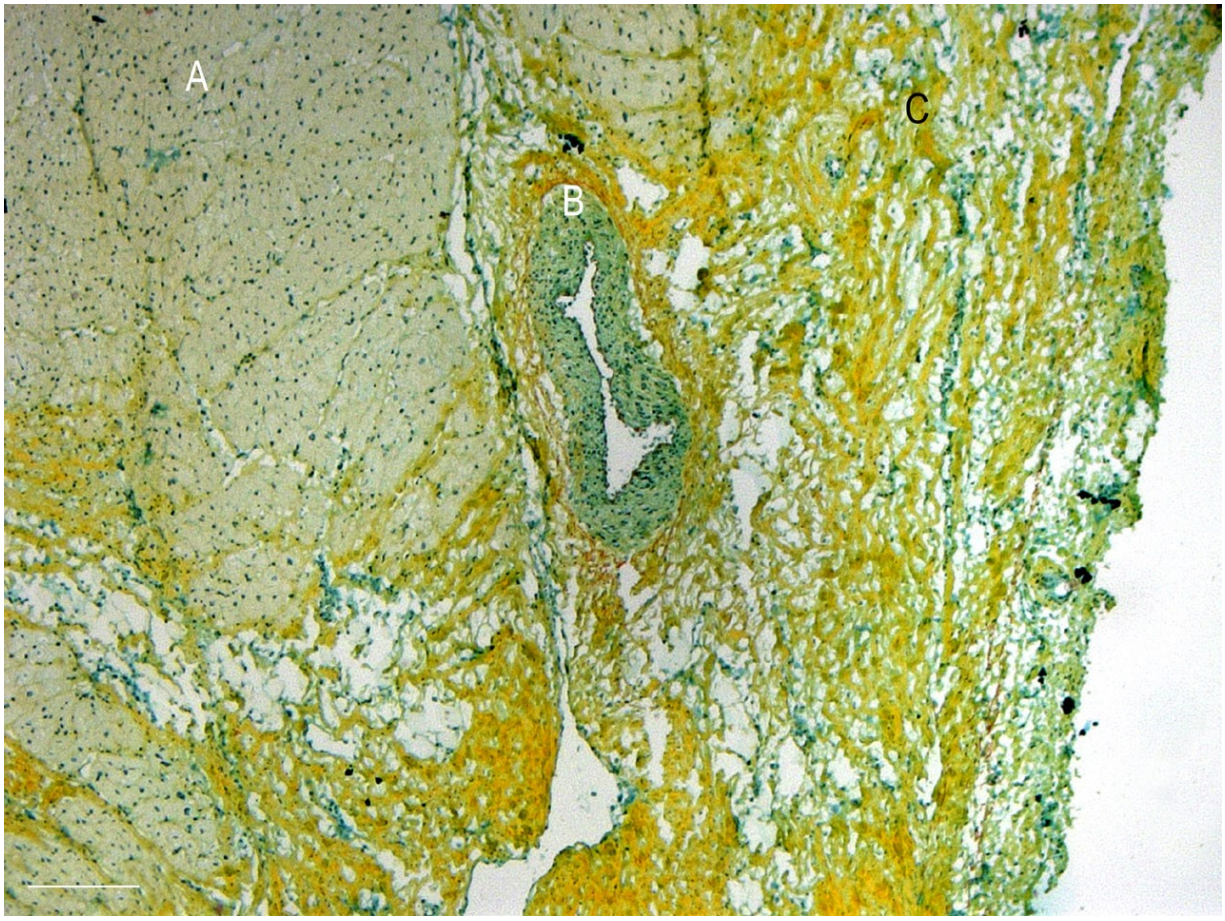

Figure 8. Border zone between myocardium, decellularized pericardium, and vascularized gastric patch. A: myocardium; B: small vein; C: gastric/pericardium patch. Pentachrome staining. Bar indicates 200 μm.

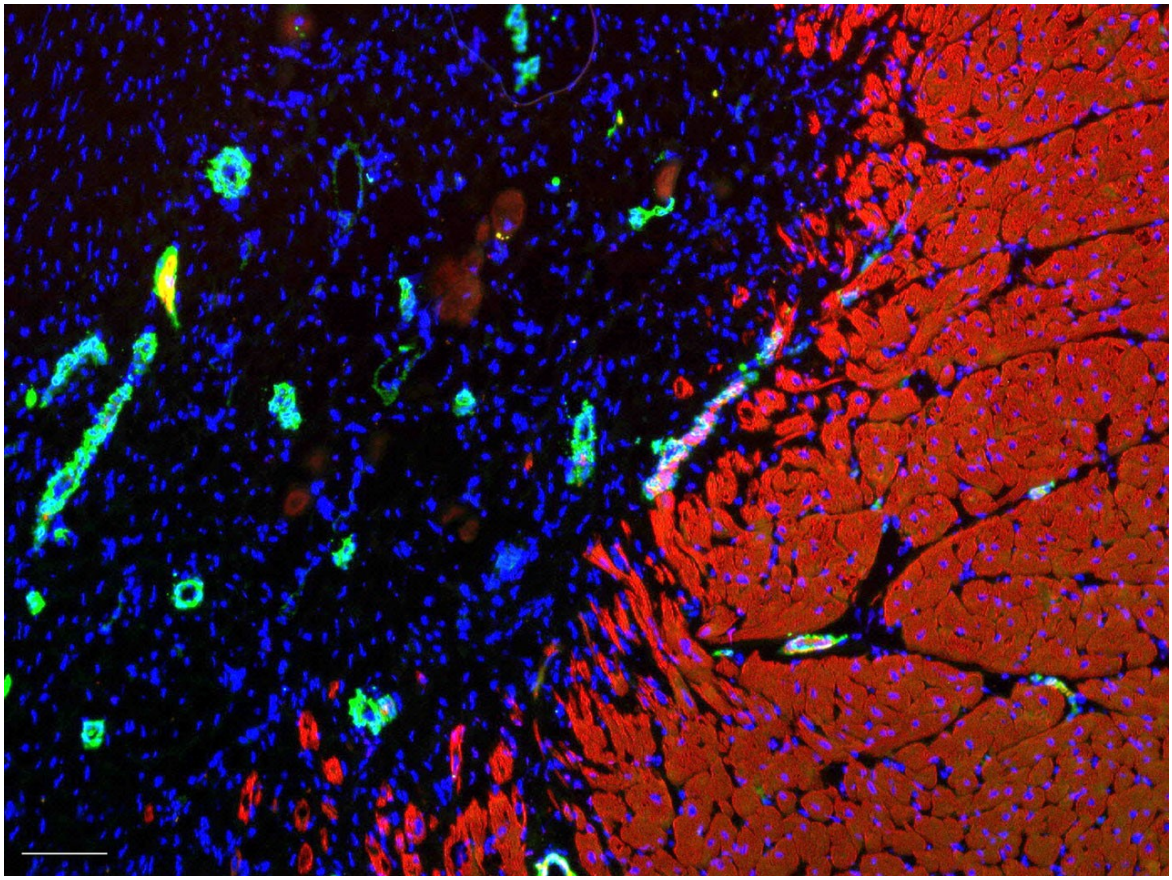

Figure 9. Border zone between myocardium (stained with troponin T, red) and vascularized gastric patch (smooth muscle actin, green, all nuclei stained in DAPI (blue)). Immunohistochemistry. Bar indicates 100 µm.

4. Discussion

Heart failure is associated with high physiological and psychological stress for patients and a severely impaired quality of life. General performance limitations, shortness of breath, edema, and life-threatening cardiac arrhythmias are just some of the serious physical symptoms of this common disease. The limited physical possibilities, the possible inability to pursue previous work, and the permanent fear of a further, life-threatening disease progression also affect psychological well-being to a considerable extent. Especially in patients with dilated cardiomyopathy, resecting the dysfunctional area of the myocardium and reconstructing the physiological volume and geometry of the ventricle can alleviate the symptoms [18]. The surgical reconstruction requires patch materials in most cases. However, the myocardial prostheses, such as Dacron, Teflon, and fixed xenogeneic pericardium, used to date are non-viable scaffolds and have no regenerative potential. They do not contribute actively to the contraction of the heart muscle, so a complete functional regeneration of the myocardium has not been reported yet. Hence, attempts have been made to engineer either natural or synthetic regenerative biomaterials [19]. As the new field of 3D bioprinting has emerged recently, the printing of contractile and functional cardiac tissue constructs is on the rise [20]. In particular, 3D bioprinting seems promising to overcome the increasing need for biomimetic scaffolds that allow for cell adhesion and immigration in the demanding field of left ventricular myocardial reconstruction [21].

Although innovative biological patch materials have the potential for physiological remodeling, in most cases, they are not suitable for a full-wall left ventricular reconstruction of the myocardium, because those tissues often are not mechanically stable enough to withstand high-pressure loads [22]. This holds true especially in the left ventricle during

the initial phase after implantation before an in vivo remodeling occurs. Zivkovic et al., therefore, used a double layer of decellularized small intestine submucosa (Proxicor) as an endoventricular cardiac patch [23]. In the present study, a left ventricular transmural defect of the myocardium was primarily covered with decellularized allogeneic pericardium before a piece of the autologous vascularized stomach was fixed transdiaphragmatically on top of the pericardium graft. This approach was based on the assumption that the pericardium decreases the high pressure from the left ventricle. Consequently, the transplanted stomach segment as the actual graft would be spared from dilation or rupture. It was expected that the heterotopically applied gastrointestinal tissue could physiologically adapt to its new function under moderate pressure conditions.

Fixed bovine or equine pericardium next to native autologous pericardium is used as a prosthetic material in cardiovascular surgery. Even kangaroo pericardium has been studied regarding its biomechanical properties and degenerative behavior [24]. To date, porcine pericardium has rarely been used as a prosthetic material. However, based on electron microscopic comparisons with bovine pericardium [25] and mechanical tests [26], porcine pericardium can be considered a possible substrate for bioartificial prostheses. Although the common fixing tanning of animal pericardium reduces its antigenicity and eliminates potentially transmissible pathogens, the fixed pericardium is no longer vital and, thus, is incapable of growth or regenerative conversion.

For this reason, there are numerous approaches to decellularizing pericardium, thus providing a substrate for in vivo or in vitro repopulation following the principles of tissue engineering. Known methods for the decellularization of xenogeneic pericardium involve detergents such as sodium deoxycholate or enzyme solutions such as trypsin. The goal is to remove cells from the graft while preserving the extracellular matrix for later reseeding. Although the combination of trypsin and EDTA has frequently been used for decellularization [27], enzyme treatment leads to a considerable deterioration of the collagen architecture of the pericardium as well as the complete removal of the basal membrane [17], which is confirmed in this study. Under these conditions, the desired immigration and adhesion of cardiomyocytes, endothelial cells, and functional connective tissue cells are questionable. Ultimately, some thrombogenicity of the enzymatically degraded tissue surface can be assumed.

In contrast, after incubating the porcine pericardium in detergents, we found minimal destruction of the collagen architecture parallel to extensive acellularity. The current study's findings correspond to those of previous studies [17] and some of the results of Dohmen et al., who decellularized equine pericardium to engineer aortic bioprostheses with a large diameter [28]. Cebotari et al. demonstrated the growth potential of heart valve prostheses that were decellularized using a similar protocol with detergents based on the in vivo reseeding of implanted acellular grafts [29]. In the present study, we also demonstrated the physiologically scarred integration of allogeneic pericardial grafts, which resulted in good clinical results in our porcine model. Nevertheless, future studies need to be carried out to investigate hosts' reactions to xenogeneic decellularized substrates that would be available for therapeutic use in almost unlimited amounts.

The transplanted autologous vascularized stomach segment showed good biological integration and viability. Supply by diffusions with nutrients and oxygen would have been barely possible through the pericardial patch and considering the diameter of the stomach wall. In this respect, the native vascular supply via the gastroepiploic artery and vein is essential for the viability of the graft.

Ultimately, the combination of the pericardium and the stomach was mechanically stable enough to prevent graft rupture in the early stage after the full-wall surgical reconstruction of the left ventricle and before the onset of scarred conversion. This improved mechanical stability facilitates the use of vascularized stomach tissue for left ventricular application. Employing the gastric patch as a prosthesis for full-wall left ventricular myocardial reconstruction in a swine model without any stabilizing support structure led to occasional aneurysm formation in previous experiments [30]. Because of the high pressure

in the left ventricle and the inherent risk of rupture or aneurysms in delicate biological prostheses, regenerative grafts have only been applied to the right ventricle or atrium [7,9]. In most cases, the patches were fixed only epicardially on ischemic zones of the left ventricular myocardium. The objective of epicardial fixation in those studies was to achieve better endogenous regeneration through cell proliferative factors and optimized vascularization in the scar tissue [8,31–36]. Another approach is the employment of pluripotent stem cells. The engraftment of stem cells or differentiated cardiomyocytes is attempted for better contractility of the infarcted myocardium [37]. However, none of the preclinical or clinical concepts has shown the feasibility of a transmural left ventricular repair. In contrast, the study at hand exceeds the epicardial surgical and cell infiltration concepts by reconstructing a full-wall left ventricular myocardial defect.

Limitations

The method presented in this study for reconstructing left ventricular transmural defects is a feasibility test. Larger test numbers are needed to confirm the positive results in a series. Second, comparative controlled studies should be performed to ascertain whether the extensive full-wall replacement of lesioned myocardium with regenerative materials yields the expected advantages over reconstructive surgery with non-vital or synthetic tissue. Finally, the use of allogeneic pericardium in this study could have led to better results than the implantation of xenogeneic substrates could achieve in a clinical scenario.

5. Conclusions

The decellularization of biological tissues as a substrate for tissue engineering is an established process. Decellularization of porcine pericardium with DOA can be an effective yet gentle procedure, as shown in this study. The positive clinical results of this project's unique method and its applicability even in the high-pressure area of the left heart give cause to consider a broad range of biological prostheses for reconstructing the myocardium. The additional stabilization of these grafts with supporting tissue such as decellularized pericardium appears to catalyze the applicability of promising regenerative bioprostheses, even for full-wall left ventricular reconstruction.

Author Contributions: A.H., S.C. and T.S. conceived the basic concept of the surgical method; M.T., T.K. and T.S. conceptualized and carried out the decellularization of the pericardium; G.B., M.T., T.K. and T.S. performed the histological analysis of the decellularization experiments; S.C., I.T., T.K. and T.S. executed the animal surgery; T.M. and I.N. developed the protocols and methodology for pre-, peri-, and postoperative animal care and managed the application for the approval of the animal experiments from the competent authorities; T.M. assessed the clinical findings during the long-term observation period in this study; D.H. and F.W. designed, planned, and executed the protocols for the magnetic resonance investigations of the test animals and assessed and interpreted the radiologic findings with regard to the clinical and surgical results in discussion with A.H., S.C., I.T., T.K., T.M., I.N. and T.S; G.B. and T.M. investigated the explanted grafts histologically; T.M. and T.S. wrote the manuscript with support from G.B., D.H., I.N., S.C. and A.H. All authors have read and agreed to the published version of the manuscript.

Funding: The project was funded by the German Research Foundation (DFG) (SFB599, R7).

Institutional Review Board Statement: The experiment was conducted in accordance with the European Convention for livestock and approved by the competent authority (LAVES, Lower Saxony) following § 8 paragraph 1 of the Animal Welfare Act BGB 1. IS 01484 (experiment #13/1180). Animal surgery was performed according to the ARRIVE guidelines [38].

Informed Consent Statement: Not applicable.

Data Availability Statement: Not applicable.

Acknowledgments: The excellent technical support of Klaus Höffler; Petra Ziehme; Astrid Dierks-Ketterkat; and Rosi Katt of the Department of Cardiovascular, Thoracic, and Transplantation Surgery; as well as Astrid Österreich and Frank Schröder of the Institute for Radiology of Hannover Medical School, is highly appreciated. We are also grateful to Andre Bleich, Klaus Otto, Karl-Heinz Napierski, and Paul Zerbe of the Central Animal facility of Hannover Medical School for their competent support in performing the animal surgery and providing excellent laboratory infrastructure. Finally, we thank the German Research Foundation (SFB599, project R7) for funding this project.

Conflicts of Interest: The authors declare no conflict of interest. The German Research Foundation, as the funder, had no role in the design of the study; in the collection, analyses, or interpretation of data; in the writing of the manuscript; or in the decision to publish the results.

References

1. Groenewegen, A.; Rutten, F.H.; Mosterd, A.; Hoes, A.W. Epidemiology of heart failure. *Eur. J. Heart Fail.* **2020**, *22*, 1342–1356. [CrossRef] [PubMed]
2. Dor, V.; Saab, M.; Coste, P.; Kornaszewska, M.; Montiglio, F. Left ventricular aneurysm: A new surgical approach. *Thorac. Cardiovasc. Surg.* **1989**, *37*, 11–19. [CrossRef] [PubMed]
3. Buckberg, G.D. Form versus disease: Optimizing geometry during ventricular restoration. *Eur.J.Cardiothorac. Surg.* **2006**, *29* (Suppl. 1), S238–S244. [CrossRef]
4. David, T.E. The use of pericardium in acquired heart disease: A review article. *J. Heart Valve Dis.* **1998**, *7*, 13–18.
5. David, T.E.; Feindel, C.M.; Ropchan, G.V. Reconstruction of the left ventricle with autologous pericardium. *J. Thorac. Cardiovasc. Surg.* **1987**, *94*, 710–714. [CrossRef] [PubMed]
6. Schilling, T.; Cebotari, S.; Tudorache, I.; Haverich, A. [Tissue engineering of vascularized myocardial prosthetic tissue. Biological and solid matrices]. *Chirurg* **2011**, *82*, 319–324. [CrossRef] [PubMed]
7. Tudorache, I.; Kostin, S.; Meyer, T.; Teebken, O.; Bara, C.; Hilfiker, A.; Haverich, A.; Cebotari, S. Viable vascularized autologous patch for transmural myocardial reconstruction. *Eur. J. Cardiothorac. Surg.* **2009**, *36*, 306–311. [CrossRef]
8. Ruel, M.A.; Sellke, F.W.; Bianchi, C.; Khan, T.A.; Faro, R.; Zhang, J.P.; Cohn, W.E. Endogenous myocardial angiogenesis and revascularization using a gastric submucosal patch. *Ann. Thorac. Surg.* **2003**, *75*, 1443–1449. [CrossRef]
9. Badylak, S.F.; Kochupura, P.V.; Cohen, I.S.; Doronin, S.V.; Saltman, A.E.; Gilbert, T.W.; Kelly, D.J.; Ignotz, R.A.; Gaudette, G.R. The use of extracellular matrix as an inductive scaffold for the partial replacement of functional myocardium. *Cell Transplant.* **2006**, *15*, S29–S40. [CrossRef]
10. Wei, H.J.; Chen, S.C.; Chang, Y.; Hwang, S.M.; Lin, W.W.; Lai, P.H.; Chiang, H.H.K.; Hsu, L.F.; Yang, H.H.; Sung, H.W. Porous acellular bovine pericardia seeded with mesenchymal stem cells as a patch to repair a myocardial defect in a syngeneic rat model. *Biomaterials* **2006**, *27*, 5409–5419. [CrossRef]
11. Hubbell, J.A. Matrix Effects. In *Principles of Tissue Engineering*; Langer, R., Vacanti, J.P., Eds.; Academic Press: San Diego, London, 2000; pp. 237–250.
12. Meredith, J.E., Jr.; Fazeli, B.; Schwartz, M.A. The extracellular matrix as a cell survival factor. *Mol Biol Cell* **1993**, *4*, 953–961. [CrossRef] [PubMed]
13. Cebotari, S.; Mertsching, H.; Kallenbach, K.; Kostin, S.; Repin, O.; Batrinac, A.; Kleczka, C.; Ciubotaru, A.; Haverich, A. Construction of autologous human heart valves based on an acellular allograft matrix. *Circulation* **2002**, *106*, I63–I68. [CrossRef] [PubMed]
14. Cebotari, S.; Tudorache, I.; Jaekel, T.; Hilfiker, A.; Dorfman, S.; Ternes, W.; Haverich, A.; Lichtenberg, A. Detergent decellularization of heart valves for tissue engineering: Toxicological effects of residual detergents on human endothelial cells. *Artif Organs* **2010**, *34*, 206–210. [CrossRef] [PubMed]
15. Heine, J.; Schmiedl, A.; Cebotari, S.; Karck, M.; Mertsching, H.; Haverich, A.; Kallenbach, K. Tissue engineering human small-caliber autologous vessels using a xenogenous decellularized connective tissue matrix approach: Preclinical comparative biomechanical studies. *Artif. Organs* **2011**, *35*, 930–940. [CrossRef]
16. Lichtenberg, A.; Tudorache, I.; Cebotari, S.; Ringes-Lichtenberg, S.; Sturz, G.; Hoeffler, K.; Hurscheler, C.; Brandes, G.; Hilfiker, A.; Haverich, A. In vitro re-endothelialization of detergent decellularized heart valves under simulated physiological dynamic conditions. *Biomaterials* **2006**, *27*, 4221–4229. [CrossRef]
17. Velivassis, M. Vergleichende Morphologische Analyse von Bovinem und Porcinem Perikard nach Dezellularisierung mit Natrium-Desoxycholat und Trypsin. Medizinische Hochschule Hannover: Hannover, Germany, 2006.
18. Calafiore, A.M.; Iaco, A.L.; Abukoudair, W.; Penco, M.; Di, M.M. Left ventricular surgical remodeling after the STICH trial. *Thorac. Cardiovasc. Surg.* **2011**, *59*, 195–200. [CrossRef]
19. Esmaeili, H.; Patino-Guerrero, A.; Hasany, M.; Ansari, M.O.; Memic, A.; Dolatshahi-Pirouz, A.; Nikkhah, M. Electroconductive biomaterials for cardiac tissue engineering. *Acta Biomater.* **2022**, *139*, 118–140. [CrossRef]
20. Wang, Z.; Wang, L.; Li, T.; Liu, S.; Guo, B.; Huang, W.; Wu, Y. 3D bioprinting in cardiac tissue engineering. *Theranostics* **2021**, *11*, 7948–7969. [CrossRef]

21. Wang, Z.; Lee, S.J.; Cheng, H.J.; Yoo, J.J.; Atala, A. 3D bioprinted functional and contractile cardiac tissue constructs. *Acta Biomater.* **2018**, *70*, 48–56. [CrossRef]
22. McCready, R.A.; Kiell, C.S.; Chugh, A.R.; Rapp, B.M.; Webb, T.H.; Barksdale, A.; Parikshak, M.; Gerdisch, M.W. Long-term Results With CorMatrix Extracellular Matrix Patches After Carotid Endarterectomy. *J. Surg. Res.* **2021**, *262*, 21–26. [CrossRef]
23. Zivkovic, I.; Mihajlovic, V.; Zdravkovic, D.; Krstic, D.; Krasic, S.; Lesanovic, J.; Peric, M.; Milacic, P. Surgical Reconstruction of a Left Ventricular Aneurysm Using an Extracellular Matrix Patch. *Braz. J. Cardiovasc. Surg.* **2022**, *37*, 259–262. [CrossRef] [PubMed]
24. Neethling, W.M.; Cooper, S.; Van Den Heever, J.J.; Hough, J.; Hodge, A.J. Evaluation of kangaroo pericardium as an alternative substitute for reconstructive cardiac surgery. *J.Cardiovasc. Surg.* **2002**, *43*, 301–306.
25. Fentie, I.H.; Allen, D.J.; Schenck, M.H.; Didio, L.J. Comparative electron microscopic study of bovine, porcine and human parietal pericardium, as materials for cardiac valve bioprostheses. *J. Submicrosc. Cytol.* **1986**, *18*, 53–65. [PubMed]
26. Garcia Paez, J.M.; Carrera, A.; Herrero, E.J.; Millan, I.; Rocha, A.; Cordon, A.; Sainz, N.; Mendez, J.; Castillo-Olivares, J.L. Influence of the selection of the suture material on the mechanical behavior of a biomaterial to be employed in the construction of implants. Part 2: Porcine pericardium. *J. Biomater. Appl.* **2001**, *16*, 68–90. [CrossRef] [PubMed]
27. Crapo, P.M.; Gilbert, T.W.; Badylak, S.F. An overview of tissue and whole organ decellularization processes. *Biomaterials* **2011**, *32*, 3233–3243. [CrossRef]
28. Dohmen, P.M.; da Costa, F.; Lopes, S.V.; Vilani, R.; Bloch, O.; Konertz, W. Successful implantation of a decellularized equine pericardial patch into the systemic circulation. *Med. Sci. Monit. Basic Res.* **2014**, *20*, 1–8. [CrossRef]
29. Cebotari, S.; Lichtenberg, A.; Tudorache, I.; Hilfiker, A.; Mertsching, H.; Leyh, R.; Breymann, T.; Kallenbach, K.; Maniuc, L.; Batrinac, A.; et al. Clinical application of tissue engineered human heart valves using autologous progenitor cells. *Circulation* **2006**, *114*, I132–I137. [CrossRef]
30. Schilling, T.; Meyer, T.; Brandes, G.; Hartung, D.; Tudorache, I.; Nolte, I.; Wacker, F.; Hilfiker, A.; Hoeffler, K.; Haverich, A.; et al. Left Ventricular Wall Reconstruction with Autologous Vascularized Gastric Graft in a Porcine Pilot Model. *Eur. Surg. Res.* **2022**. [CrossRef]
31. Huang, W.; Zhang, D.S.; Millard, R.W.; Wang, T.; Zhao, T.M.; Fan, G.C.; Ashraf, A.; Xu, M.F.; Ashraf, M.; Wang, Y.G. Gene manipulated peritoneal cell patch repairs infarcted myocardium. *J. Mol. Cell. Cardiol.* **2010**, *48*, 702–712. [CrossRef]
32. Tan, M.Y.; Zhi, W.; Wei, R.Q.; Huang, Y.C.; Zhou, K.P.; Tan, B.; Deng, L.; Luo, J.C.; Li, X.Q.; Xie, H.Q.; et al. Repair of infarcted myocardium using mesenchymal stem cell seeded small intestinal submucosa in rabbits. *Biomaterials* **2009**, *30*, 3234–3240. [CrossRef]
33. Taheri, S.A.; Yeh, J.; Batt, R.E.; Fang, Y.; Ashraf, H.; Heffner, R.; Nemes, B.; Naughton, J. Uterine myometrium as a cell patch as an alternative graft for transplantation to infarcted cardiac myocardium: A preliminary study. *Int. J. Artif. Organs* **2008**, *31*, 62–67. [CrossRef] [PubMed]
34. Taheri, S.A.; Ashraf, H.; Merhige, M.; Miletich, R.S.; Satchidanand, S.; Malik, C.; Naughton, J.; Zhao, Q. Myoangiogenesis after cell patch cardiomyoplasty and omentopexy in a patient with ischemic cardiomyopathy. *Tex. Heart Inst. J.* **2005**, *32*, 598–601. [PubMed]
35. Kusaba, E.; Schraut, W.; Sawatani, S.; Jaron, D.; Freed, P.; Kantrowitz, A. A diaphragmatic graft for augmenting left ventricular function: A feasibility study. *Trans. Am. Soc. Artif. Intern. Organs* **1973**, *19*, 251–257. [CrossRef] [PubMed]
36. Beck, C.S. The development of a new blood supply to the heart by operation. *Ann.Surg.* **1935**, *102*, 801–813. [CrossRef]
37. Broughton, K.M.; Sussman, M.A. Cardiac tissue engineering therapeutic products to enhance myocardial contractility. *J. Muscle Res. Cell Motil.* **2020**, *41*, 363–373. [CrossRef]
38. Percie du Sert, N.; Hurst, V.; Ahluwalia, A.; Alam, S.; Avey, M.T.; Baker, M.; Browne, W.J.; Clark, A.; Cuthill, I.C.; Dirnagl, U.; et al. The ARRIVE guidelines 2.0: Updated guidelines for reporting animal research. *BMJ Open Sci.* **2020**, *4*, e100115. [CrossRef]